Adaptive GNSS Receiver Design for Highly Dynamic Multipath Environments

ARIF HUSSAIN[1], ARSLAN AHMED[1], HINA MAGSI[1], AND RAJESH TIWARI[2,3]

[1]GNSS and Space Weather Laboratory, Department of Electrical Engineering, Sukkur IBA University, Sukkur 65200, Pakistan
[2]Nottingham Scientific Limited (NSL), Nottingham NG7 2TU, U.K.
[3]Department of Electrical and Electronic Engineering, University of Nottingham, Nottingham NG7 2RD, U.K.

Corresponding author: Arslan Ahmed (arslan.ahmed90@gmail.com)

ABSTRACT Ubiquitous navigation requires timely, uninterrupted and accurate estimate of receiver's position at all times, in all environments and for all modes of transportation and it is highly dependent on satellite availability, geometry and accurate positioning estimation. However, the availability, continuity and accuracy of a GNSS can be severely affected in a highly dynamic environment due to blockage, fading and multipath. This results in positioning information inaccurate, unreliable and sometimes unavailable. This paper presents a study on the potential vulnerabilities that can affect a multi-constellation multi-frequency GNSS receiver in low to highly dynamic multipath environments such as clear line-of-sight, partially and highly obstructed environments to characterize the distortions/anomalies which could significantly affect the satellite signals and their impact on positioning and navigation. The multi-constellation multi-frequency GNSS receiver configuration in this paper is set to GPS, GLONASS, Galileo and BeiDou for the first time at full capacity and performance comparison is made with the GPS based on satellite availability, blockage, continuity, precision and accuracy parameters. These parameters are then used in this paper to detect and characterize the type of environment for the multi-constellation GNSS receiver without using any external aiding devices or sensors. Based on environment detection and characterization, a new Adaptive Environment Navigation (AEN) based GNSS receiver design is proposed which can work in real time and has achieved an overall availability and accuracy factor of 94% in highly dynamic multipath/NLOS environment along with a reduction in the blockage coefficient, β, by almost 11% resulting in more accuracy and precision than the standard multi-constellation GNSS receiver where the availability factor was found to be 57% only.

INDEX TERMS Adaptive tracking, GNSS, accuracy, precision, navigation.

I. INTRODUCTION

The rapid urbanization in the developed/developing countries brought several challenges for the cities to cope with issues related to administrative, infrastructure, logistics and transportation. It is thus essential to make large cities more sustainable and livable whilst ensuring safety, security and health. In such a dynamic and demanding environment, accurate and reliable positioning, navigation and timing (PNT) services are essentially important to hundreds of civilians and military applications such as railways, aviation, marine navigation, road safety, policing, agriculture etc [1]–[5]. The global navigation satellite system (GNSS) can provide accurate and reliable PNT services with accuracy of a few

The associate editor coordinating the review of this manuscript and approving it for publication was Zheng H. Zhu.

centimeters in clear open-sky view by utilizing most up to date precise point positioning (PPP) techniques [6], [7]. Current standardization activities in the positioning and navigation community are paving the way for using multi-constellation GNSS as a primary means of positioning and navigation. However, in highly dynamic environments (e.g., tall building, trees, congested pathways), the availability, continuity and accuracy of GNSS may be affected due to signal blockage, fading/shadowing, multipath and interference [8]. In such environments, the satellite signals are reflected, scattered, fluctuated and sometimes completely blocked by roofs and walls of high-rise buildings, fly-over bridges and complex road scenarios, making positioning information inaccurate, unreliable and largely unavailable [9]–[12] leading to reduced navigation services or no services.

The GNSS consists of a space segment (satellites), a control and monitoring segment and a user segment (ground station/receivers). The ground-based GNSS receiver processes the received GNSS signals and estimates the travel time to extract the satellite positions (x^k, y^k, z^k) from the navigation message [13], [14]. Here, k represents the satellite number. The satellite positions are then used to estimate the distance between the receiver and k^{th} satellite which is also known as the pseudorange. The pseudoranges from different satellites gives the final estimate of the user position (x, y, z) [15]. There exist several GNSS based positioning techniques for improved accuracy such as standard GNSS, DGNSS, RTK, SBAS, PPP etc. The comparison is shown in Fig. 1.
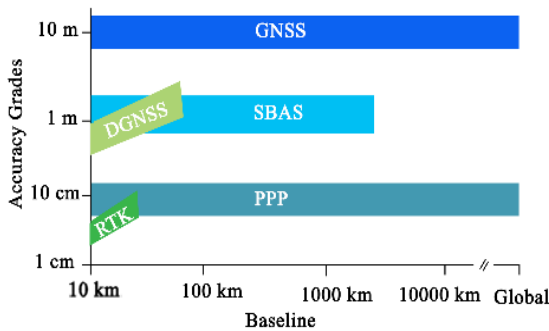

FIGURE 1. Comparison of positioning accuracies provided by RTK, PPP, SBAS, DGNSS and Standard GNSS methods.

The precise point positioning (PPP) is preferred over others as it provides users with highly precise and accurate positioning by using dual-frequency pseudo-range and carrier phase measurements together with additional ephemeris correction stream such as precise satellite orbit and clock products to equate or model certain errors [16], [17]. A comparison between the standard positioning service and PPP is shown in Fig. 2. In PPP, errors due to tropospheric delay, ionospheric delay, clock biases, multipath (MP) and other measurement noises need to be carefully handled and equalized.
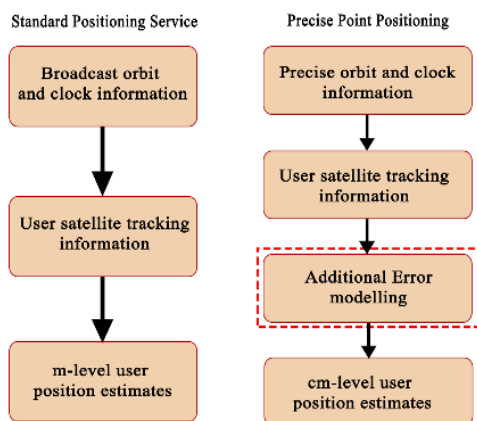

FIGURE 2. Difference between the Standard Positioning and Precise Point Positioning.

Most of the errors mentioned above are almost deterministic in nature and can be equalized by available mitigation models [18]–[21]. However, dealing with MP/NLOS errors is practically difficult in many situations because of its nature, i.e., high dynamics and randomness. Several studies have suggested detection, modelling and mitigation techniques for multipath signals at various levels such as antenna, receiver and measurement or position [22]–[28]. In [22] and [23], some common techniques to mitigate multipath have been discussed based on: (1) de-weighting of affected measurements; (2) using dual-polarized antenna; (3) using the vector tracking loop; (4) navigation processor based techniques which applies a consistency check to pseudorange measurements. [24] has worked on reducing the exclusion of de-weighted measurements, [25] has used sidereal filtering to extract noisy carrier phase residuals whereas [26] has focused on elevation angle and C/N_o to mitigate the multipath effects. [27], [28] have used dual polarized antenna for multipath mitigation and to improve the quality of positioning. These techniques can reduce multipath errors to some extent, but completely eliminating them in a wide range of environments is still a challenging task for navigation receivers regardless of the type of hardware/software used.

The average positioning error in case of PPP is less than one meter in clear open-sky [6]. However, this level of accuracy cannot be achieved in obstructed environments even if the receiver is equipped with additional error modelling [29], because there are significant chances of navigation services being interrupted or their performance reduced due to signal blockage and MP/NLOS [7], [9], [30] leading to inaccurate positioning solution.

Keeping in view the challenges faced by the satellite-based navigation systems, this paper presents a comprehensive study on the potential vulnerabilities that can affect the GNSS performance in low and high dynamic multipath environment such as clear open-sky view, partially degraded environment having both LOS and NLOS signals and high multipath environment having little or no LOS signal reception [31]. The paper compares the availability, accuracy, precision, continuity and quality of single constellation and multi-constellation GNSS configurations. For multi-constellation case, satellites of GPS, GLONASS, GALILEO and BeiDou are used for positioning whereas for single constellation, GPS is used. The comparison is then made through carefully selected field experiments in low, medium and high multipath environments in order to highlight the effects of signal blockage and multipath on single and multi-constellation GNSS receiver performance. A series of field experiments has been carried out with different working modes and different observation conditions using four major characteristics of a GNSS that has never been done before, i.e., Availability, Signal Characteristics, Service Continuity and Accuracy. These characteristics are studied in detail through blockage coefficient, satellite availability, loss of signal lock and standard quality (accuracy and precision) measures for positioning and navigation such as Distance Root Mean Square (DRMS),

Circular Error Probable (CEP) and Dilution of Precision (DOP). In order to improve the receiver performance in high dynamic multipath environments, an adaptive environment based navigation (AEN) algorithm is proposed which is then used in a GNSS receiver for position improvement based on environment detection and characterization. The proposed AEN based GNSS receiver model does not need any extra hardware or external aiding devices or sensors and updates the tracking loop paramters based on working environment for increasing the satellite availability and accuracy and thus the receiver performance.

The overall paper is organized as follows. Section II introduces the performance evaluation methodology adopted for single and multi-constellation systems. Sections III describes the experimental setup used for performance evaluation study whereas section IV discusses the experimental sites and observation periods used for data collection. In sections V, comparison between the single and multi-constellation GNSS receiver performance is presented. The last section, i.e., Section VI, talks about the proposed navigation receiver design based on Adaptive Environment Navigation (AEN) Algorithm.

II. PERFORMANCE EVALUATION METHODOLOGY

In order to understand the depth of problems faced by single and multi-constellation GNSS receivers in position estimation, an observation signal model must be evaluated first to account for the sources of errors in a GNSS. As already known, the GNSS signal received at the ground-based receiver is weaker than the background noise and hence is prone to several sources of noises and errors [32]–[35]. The generic form of a pseudorange equation for position estimation [36] can be expressed as

$$\rho^k = \| P^k - P_r \|_2 + \epsilon_s^k + \epsilon_{cb} + \epsilon_n + \epsilon_e^k \qquad (1)$$

where,

- ρ^k is the pseudorange between the receiver and k^{th} satellite where $k \in \{1, \ldots, N\}$ and, N is the total number of visible satellites. It should be noted that $(N \geq 4)$ in case of single constellation and changes when adding more constellations in position estimation.
- $\| P^k - P_r \|_2 = \sqrt{(x^k - x)^2 + (y^k - y)^2 + (z^k - z)^2}$ is the true distance between k^{th} satellite and receiver
- $P^k = (x^k, y^k, z^k)$ is the known k^{th} satellite position
- $P_r = (x, y, z)$ is the receiver position to be estimated
- ϵ_s^k is the error associated with k^{th} satellite due to space effects (i.e ionospheric delay and troposheric delay)
- $\epsilon_{cb} = c(dt - dT^k)$ is the error due to clock bias. Here, dt is the receiver clock bias and dT^k is the satellite clock bias. In case of using more than one constellation, inter-system biases, B_τ, must be considered, e. g., in case of using four constellations, three inter-system biases between Galileo, GLONASS and BeiDou compared to GPS (i.e., reference clock) are required.
- ϵ_e^k is the error factor associated with k^{th} satellite due to environment.

All the error sources mentioned above are almost constant and can be equalized by available mitigation models. However, ϵ_e^k is the error factor associated with k^{th} satellite due to working environment that is random and unpredictable in nature and has the most severe effects on GNSS position estimation [37]. The error due to environment alone can be can be modelled as

$$\epsilon_e^k = \epsilon_\beta + \epsilon_{NLOS/MP} + \epsilon_G \qquad (2)$$

where ϵ_β is the error due to reduced availability of satellite, $\epsilon_{NLOS/MP}$ is error associated with NLOS reception or multi-path and ϵ_G is the error due to poor geometry. After considering these errors, the final equation of pseudorange given by (1) can be rewritten as

$$\rho^k = \| P^k - P_r \|_2 + \epsilon_s^k + \epsilon_{cb} + \epsilon_n + \epsilon_\beta + \epsilon_{NLOS/MP} + \epsilon_G \qquad (3)$$

The parameters used for evaluating the GNSS performance are described below.

A. SATELLITE AVAILABILITY AND BLOCKAGE CO-EFFICIENT (β)

An accurate GNSS positioning require timely estimate of a user position at all times, in all environments and across all modes of operation and it is highly dependent on the availability and geometry of satellites [23], [38]. The satellite availability can be defined as number of satellites locked by a GNSS receiver at a particular location on a specific time and is quantified by a blockage co-efficient (β). In this paper, (β) is estimated by comparing the number of locked satellites in a specific environment under observation to a clear-open sky view environment. The observation environment can be an indoor environment, place surrounded by buildings or covered by trees having no direct access to the GNSS signals. The blockage coefficient (β) can be found as

$$\beta = 1 - \frac{VS_{avg} - BS_{avg}}{VS_{avg}} \qquad (4)$$

where, VS_{avg} is the average no. of detected satellites in clear open sky and BS_{avg} is the average number of detected satellites in observation environment in a given time interval. We have taken average number because satellites in orbit are in continuous motion, therefore, satellite availability is also a function of time.

B. CONTINUITY AND SERVICE INTERRUPTION

Safety and security critical applications require accurate, timely as well as uninterrupted estimate of PNT solution which is only possible when an adequate number of satellites are locked by a receiver in both the single constellation and multi-constellation cases. Any less than that result in outages [36], [39]. The continuity can be defined as the system's ability to operate without any interruption or failure. In this paper, the continuity is quantified by loss of signal locked by a receiver. The loss of lock depends on the signal intensity (*SI*)

which can be severely affected by the NLOS reception, multipath and/or fading. In highly dynamic environments, the signal strength can fluctuate randomly as a result of multipath, NLOS and fading making it problematic for a receiver to hold lock onto a satellite.

$$SI = \frac{10log_{10}(P_{max}) - 10log_{10}(P_{min})}{10log_{10}(P_{max}) + 10log_{10}(P_{min})} \quad (5)$$

where, P_{max} and P_{min} are maximum and minimum power levels of received signal respectively. Whenever, SI is greater than a certain level there are significant chances that a loss of lock event is likely to occur. Therefore, *SI* can be used to find out the number of times a particular satellite signal loses lock which can then be used to find the continuity factor (δ) given as

$$\delta = \frac{VS_{total} - VS_{loss}}{VS_{total}} \quad (6)$$

where, VS_{total} is the total number of visible satellites and VS_{loss} represents the total number of satellites with loss of lock events. Overall, the GNSS service will be interrupted whenever $VStotal - VSloss < N$, where N is 4 in case of single constellation and changes based on adding more constellations in position estimation, such as, in this paper, 4 systems are used for multi-constellation study, so, N will be 7.

C. PRECISION AND ACCURACY MEASURES
The efficiency of a GNSS receiver is evaluated by the precision and accuracy it provides. Accuracy refers to degree of closeness to true position while precision refers to closeness towards the mean or true position [40], [41]. Fig. 3 shows the difference between the accuracy and precision considering the center as the true or mean position.
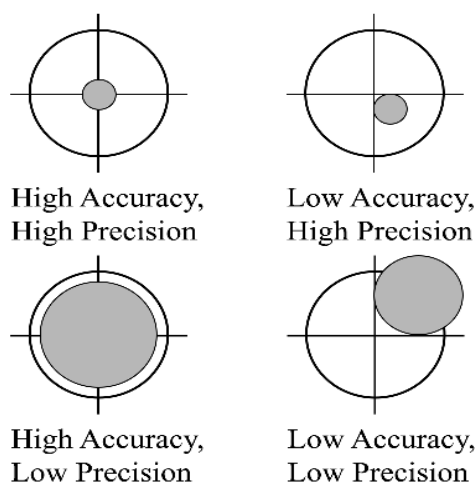
FIGURE 3. Difference between accuracy and precision in a GNSS Receiver [42].

For a stationary GNSS receiver, it is usually observed that the reported positions are scattered over certain region and this dispersion is due to the measurement errors. The accuracy

and precision are the key parameters used to analyze the efficiency of a receiver. In this paper, the precision and accuracy measurements used are discussed below.

1) ACCURACY EVALUATION
To analyze and quantify the GNSS performance, a confidence region is used to measure the accuracy. The confidence region is the radius which describes the probability that the expected outcome will be within that radius [42]. In this paper, the accuracy is estimated using the following two factors:

a: CIRCULAR ERROR PROBABLE (CEP)
CEP is the radius of a circle, centered on true/mean position, whose boundary is expected to include 50% points of total reported positions. For instance, if a CEP of 2 meters is quoted and 1000 values are estimated then 500 points /solutions will lie within 2 m circle around true/mean position also known as the confidence region. The CEP is found as

$$CEP = 0.62\sigma_x + 0.56\sigma_y \quad (7)$$

where, σ represents the standard deviation of estimated coordinates (x, y).

b: DISTANCE ROOT MEAN SQUARE (DRMS)
The DRMS is also a 2D accuracy evaluation measure computed as the square root of averaged squared position errors. In DRMS, it is expected that 65% of measured positions lie within the confidence region circle found as

$$DRMS = \sqrt{\sigma_x^2 + \sigma_y^2} \quad (8)$$

where, σ^2 is the variance of estimated coordinates (x, y). The confidence region radius is highly dependent upon positioning errors, as error increases the radius increases which results in reduced accuracy.

2) DILUTION OF PRECISION
The precision of the PNT solution reported by a GNSS receiver can be affected greatly by satellite geometry. The number as well as geometric positions of satellites in orbit contributes to position uncertainty. This is normally quantified by dilution of precision (DOP). The position DOP (PDOP) refers to positioning error caused by the relative position of the satellites and the geometry of satellites in view [43]. The effect of satellite geometry on user position based on PDOP is shown in Fig. 4. A good satellite geometry means that satellites are spread apart as shown in Fig. 4(a) giving more precise position centered around mean whereas a bad satellite geometry is shown in Fig. 4(b) leading to erroneous positions spread over a wider area around the mean position. The PDOP can be estimated using (9). A PDOP value of less than 1 means, a good satellite geometry and as PDOP value start increasing, so does the error.

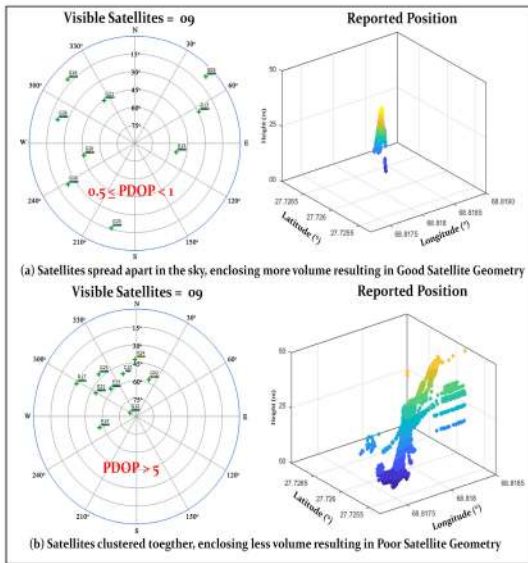$$PDOP = \sqrt{\sigma_x^2 + \sigma_y^2 + \sigma_z^2} \quad (9)$$

FIGURE 4. Effect of satellite geometry on accuary of position estimation.

III. EXPERIMENTAL SETUP

The GNSS receiver used for logging the data is Septentrio Polarx5S multi-constellation receiver connected to a choke ring B3/E6 Antenna [44], [45]. The signals locked by the Septentrio receiver for this experiment are GPS, GALILEO, GLONASS and BEIDOU. The experimental setup is shown in Fig. 5. The complete description of the GNSS signals are listed in Table 1 along with the PRN numbers used by Septentrio Polarx5s receiver for identification. Sig1 and Sig2 are used in this paper for performance evaluation study.

FIGURE 5. Experimental setup for logging the single constellation and multi-constellation GNSS data at the observation sites.

IV. EXPERIMENTAL SITES

The data collection sites is a key to understand the actual problems faced by single and multi-constellation GNSS navigation. Most of the field experiments for environment characterization are performed in urban or semi-urban or open-sky

TABLE 1. GPS, GLONASS, GALILEO and BeiDou signals description and numbers as identified in Septentrio multi-constellation GNSS receiver.

System	Satellites PRN	Sig1	Sig2	Sig3	Sig4	Sig5
GPS	1 to 31	L1CA (1575.42MHz)	L2 C (1227.60MHz)	L2 P (1227.60MHz)	L5 (1176.45MHz)	
GLONASS	37 to 61	L1CA (1602MHz)	L2 C (1246MHz)	L3 OC (1202MHz)		
GALILEO	71 to 106	E1 (1575.42MHz)	E5a (1176.45MHz)	E5b (1207.14MHz)	E5 AltBOC (1191.79MHz)	E6 (1278.75MHz)
BEIDOU	141 to 171	B1 (1561.09MHz)	B2I (1207.14MHz)	B3 (1268.52MHz)	B1C (1575.42MHz)	B2a (1176.45MHz)

environments [46]–[48] where it is difficult to use some of the parameters used above for environment characterization without knowing the exact geometry of the satellites and probability of blockage [49]. In order to precisely gauge the depth of problems faced by a GNSS receiver, carefully planned field experiments are conducted on candidate sites having high degree of naturalism. The field experiments are performed to investigate the effects of Blockage, multipath and Loss of lock etc which could severely affect a GNSS signal. For less chances of biased measurements, the field experiments are conducted during the same time interval on consecutive days.

Fig. 6(a) shows the observation sites used for the experimentation. The selected site is a building, i.e., Department of Electrical Engineering, Sukkur IBA University, Pakistan, whose inside provide a perfect NLOS/MP signal reception as it is hollow from inside. The building is a 5 story 100 feet tall building. The selected experiments are performed using the three scenarios: Fig. 6(b) is the clear open-sky view where all the satellites have clear LOS having negligible multipath without any blockage. The next site is shown in Fig. 6(c) which is the partially obstructed environment named as Half-Sky and some of the satellites are either blocked or affected by multipath. The last scenario used is the highly dynamic multipath environment named as the Quarter-sky having significant blockage and multipath as shown in 6(d). The experiments were performed in two modes, i.e., multi-constellation multi-frequency (MCMF) GNSS using GPS, GLONASS, GALILEO and BeiDou and the single constellation mode using GPS only. The complete list of the experiments performed using MCMF and SCMF modes are listed in Table 2.
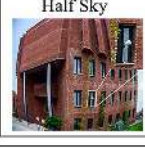
V. GNSS PERFORMANCE EVALUATION

In this paper, clear open-sky view is taken as a best possible reference scenario having direct LOS reception for almost all the satellites above 10° elevation and is then compared with the half-sky and quarter-sky environments. It should be noted that the three cases chosen here may be considered as the alternative application scenario's to such as aviation and marine navigation where there is direct LOS signal reception (open-sky); on road navigation for automobiles when only some of the satellites are blocked (half-sky) and; the navigation in dense urban environments when mostly there is no direct LOS signal available to the receiver

FIGURE 6. (a) Experimental site for single and multi-constellation GNSS data collection. (b) Antenna at the rooftop for clear open sky, (c) Partially degraded environment (Half sky), (d) Highly dynamic multipath environment (Quarter sky).

TABLE 2. Field sites, observation periods and GNSS System used for the experimentation and data collection.

Experiment	Observation Sites	Systems	Observation period (GNSS time)	Receiver Antenna
Ept1a	Open Sky	GPS+GLONASS+ Galileo+BeiDou	06:00 to 12:00 July 04,2019	Septentrio PolaRx5S
Ept1b		GPS Only	06:00 to 12:00 July 05,2019	PolaNt Choke Ring B3/E4 Antenna
Ept2a	Half Sky	GPS+GLONASS+ Galileo+BeiDou	06:00 to 12:00 July 09,2019	Septentrio PolaRx5S
Ept2b		GPS Only	06:00 to 12:00 July 11,2019	PolaNt Choke Ring B3/E4 Antenna
Ept3a	Quarter Sky	GPS+GLONASS+ Galileo+BeiDou	06:00 to 12:00 July 06,2019	Septentrio PolaRx5S
Ept3b		GPS Only	06:00 to 12:00 July 08,2019	PolaNt Choke Ring B3/E4 Antenna

(quarter-sky). In the next two sections, the constrained, limitations, availability and performance of multi-constellation and single constellation receiver configuration is discussed.

A. MCMF GNSS RECEIVER CONFIGURATION

The results of MCMF GNSS configuration in low to highly dynamic multipath environment is shown in Fig. 7. The performance is evaluated based on the satellite geometry, availability, precision and accuracy. The observation period of the experiment was 06:00 to 12:00 hours UTC performed over consecutive multiple days as mentioned earlier. Fig. 7(a) shows the geometric distribution of satellites represented by the sky-plot which shows the actual locations of the satellites in sky with respect to elevation angle. The +ve sign in Fig. 7(a) represents the locked satellites whereas its color represents the navigation system. The purple color shows the
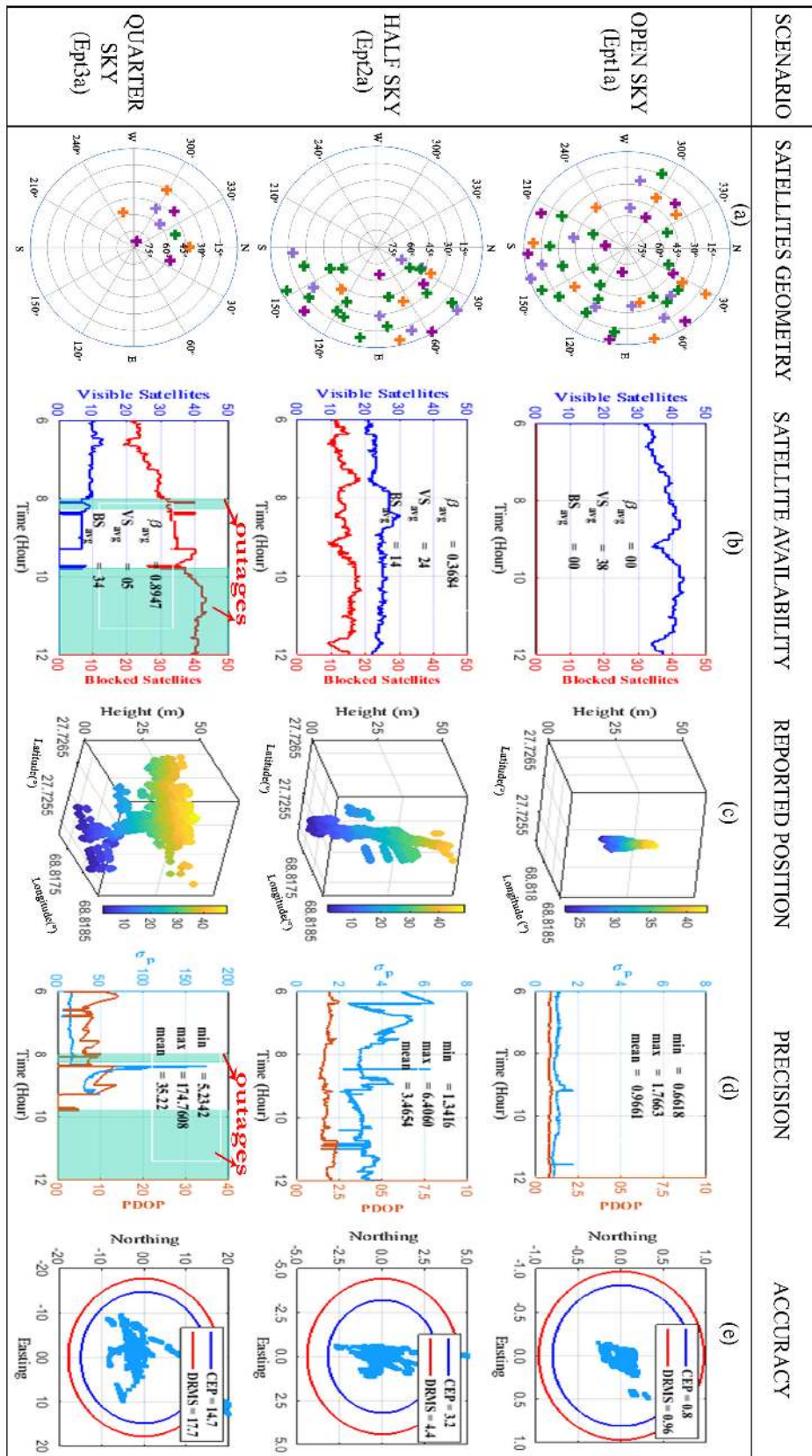
FIGURE 7. Multi-constellation GNSS Performance in open-sky, half-sky and quarter-sky: (a) Geometric distribution of satellites in orbit; (b) Satellite availability; (c) Reported position using latitude, longitude and height); (d) Precision in PDOP and σ_P; (e) Accuracy (CEP and DRMS).

GPS satellites, green is assigned to BeiDou, blue represents the Galileo and orange color shows the GLONASS satellites. Fig. 7(b) shows the locked/visible vs blocked satellite status. Fig. 7(c) shows the position using latitude, longitude and height for 6 hours observation period. Fig. 7(d) shows the position standard deviation and PDOP and Fig. 7(e) shows the CEP and DRMS plotted on a northing easting plane.

In Fig. 7(a), in case of open sky, satellites are spread over whole sky having a good satellite geometry. However, in Half-Sky and Quarter-Sky cases, all of the satellites are concentrated on one side or another due to blockage making some of the satellites undetected even though they are present in the radio-vicinity. The satellites geometry and accuracy are inter-linked because the better the geometric distribution of satellites will be the better will be the positioning accuracy. The next metric used for the performance evaluation of the multi-constellation GNSS is the satellite availability shown in Fig. 7(b). The satellite availability is quantified by the blockage factor β. In open-sky environment, blockage factor is considered zero because there is no obstruction and maximum number of satellites were locked by the receiver during the observation period $(6:00 - 12:00)$ at any given time. On average, 38 satellites were locked however, the number vary between 32 and 43 and this is due to the movements of satellites in orbit around the Earth and elevation angle. The satellites availability is highly correlated with precision and accuracy which shows the increase in positioning standard deviation in Fig. 7(d) when the locked satellites dropped to 33 at around 09:00 and 11:50 hours. In case of partially degraded environment (Half-sky), the average number of locked satellites reduced from 38 to 24 and the blockage factor increased by 36.84% leading to more errors in the positioning solution. The same was the case with the highly degraded environment (Quarter-Sky) having a blockage factor of 0.8684 in which the position was further degraded as can be seen in Fig. 7(c). It should be noted that in quarter-sky case, due to MP/ NLOS reception from the satellites, there were less than 7 satellites locked at around 08:00 hours and between 09:45 to 12:00 hours having no positioning solution available during this time as marked by outage regions in Fig. 7(b).

Once the satellite geometry and availability is checked, position is then estimated for the open-sky, half-sky and quarter-sky cases as shown in the top, middle and bottom graphs of Fig. 7(c) respectively. As expected, although the receiver is a stationary one but the half-sky and quarter-sky cases are showing a great deal of variations in the reported positions as compared to the open sky case. The dispersion in reported positions, which are more scattered around the mean in half-sky and quarter-sky cases in Fig. 7(c), is due to reduced precision and accuracy which is shown in Fig. 7(d) and Fig. 7(e) respectively. To estimate the error in the reported positions, the standard deviation of the coordinates x, y, z or (Latitude, Longitude, Height) is taken, i.e., $\sigma = \frac{\sqrt{\sigma_x^2} + \sqrt{\sigma_y^2} + \sqrt{\sigma_z^2}}{3}$ which is shown in Fig. 7(d) along

with the PDOP. The mean of σ is found to be around 1m in case of open-sky case which increases up to 3.4 m and 35.2 m in case of half-sky and quarter-sky cases. The purpose of showing the PDOP and σ on the same graph is to show the effect of PDOP on positioning error. In case of open-sky, the PDOP is mostly less than 1 having a little effect on the positioning error. However, the PDOP has a severe effect in half-sky and quarter-sky cases having average PDOP values of around 2.3 and 9 respectively. So, apart from other factors, the satellite geometry has a major influence on the positioning error which cannot be neglected. The statistical accuracy (CEP and DRMS) estimated in all three candidate sites is shown in Fig. 7 (e). Whenever, there is a mention of accuracy about a GNSS receiver then it means that it is the CEP value and is sometimes also mentioned by DRMS. In case of open-sky, the radiuses of CEP and DRMS circles were found to be 0.8 m and 0.96 m respectively. Infact, in open-sky case, almost 95% of the values were found to be within 0.3m radius of the true/mean position. In case of half-sky, the radiuses of CEP and DRMS increases to 3.2 m and 4.4 m respectively representing that the estimated position has scattered over a larger area and there is a probability that 50% of the reported positions may have an error of more than 3.2 m although we found that more than 95% of the reported positions were within the confidence regions of the CEP and DRMS as marked by blue and red circles respectively. This error further increased in the case of quarter-sky as shown in Fig. 7(e) where the CEP and DRMS radiuses increased to 14.7 m and 17.7 m respectively which are quite large and may be a problem for the receiver to navigate correctly. The overall results of multi-constellation configuration presented in Fig. 7 for all the candidate sites are summarized in Table 3. The table gives a summarized overview of how the GNSS accuracy and precision can be affected from low to highly obstructed environment.

TABLE 3. Summary of the MCMF GNSS receiver configuration in Open-Sky, Half-sky and Quarter-sky.

Scenario	Satellite Availability		Precision		Accuracy	
	VS mx/ag/mn	BS mx/ag/mn	σ_p mx/ag/mn	PDOP mx/ag/mn	CEP (m)	DRMS (m)
Open Sky	43/38/32	00/00/00	1.76/0.96/0.6	0.96/0.79/0.71	0.8082	0.9690
Half Sky	30/24/20	19/14/09	6.41/3.46/1.34	2.42/1.77/1.23	3.2044	4.4136
Quarter Sky	12/05/05	36/34/23	174.7/35.2/5.23	11.2/3.42/2.73	14.7	17.7

VS = Visible Satellites, BS = Blocked Satellites, σ_p = Position Standard Deviation, mx = maximum, ag = average, mn = minimum

In order to single out how the signal locked by the MCMF GNSS receiver in quarter-sky actually looks like and how the service is interrupted, signal intensity and lock status of some of the satellites from GPS, GLONASS, Galileo and BeiDou are shown in Fig. 8 having visibility time of almost half an hour. A signal is likely to lose lock whenever the
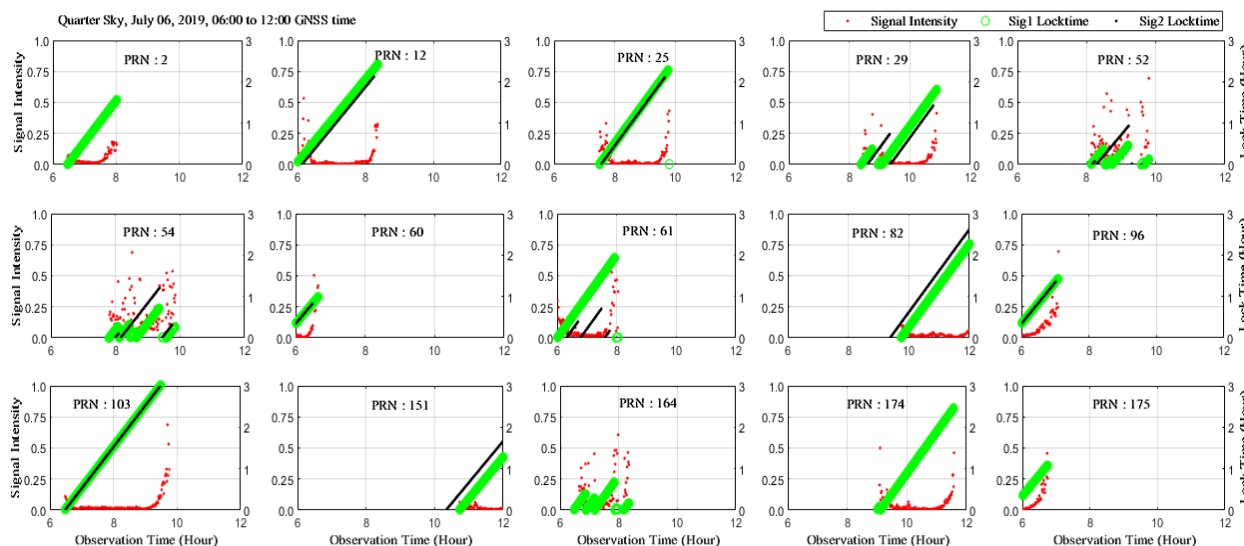
FIGURE 8. Signal intensity variations and lock time observed at Sig1 and Sig2 of the MCMF GNSS receiver in highly dynamic multipath Quarter sky case.

signal intensity variations are greater than 0.3. The lock time is shown for Sig1 and Sig2 used for positioning. It can be seen in Fig. 8 that most of the satellites having greater variations of signal intensity have lost lock to the receiver and gone for re-acquisition. In Fig. 7, it is shown that the system has gone to outage after 09:45 hours in the quarter-sky case due to inadequate number of satellites available. This can be verified from Fig. 8 in which there were less than 7 satellite signals locked by the receiver during that time and in case they were locked then loss of lock was frequently occurring such as in the case of PRN:29, PRN:52 and PRN:54 due to which the receiver was unable to provide any positioning service.

The above results of MCMF receiver configuration shows that the positioning estimation using a combination of multiple navigation systems still may not guarantee an accurate and precise position in case of highly dynamic multipath/NLOS environments although, it may help in selecting satellites with strong signal strength and good geometry from a pool of available satellites which can be helpful in partially obstructed cases or no obstruction. The point to be mentioned here is that highly dynamic multipath environments are mostly dense urban areas where standalone GNSS services has always resulted in no service or reduced accuracy and large errors if no aiding device is used in position estimation.

B. SINGLE CONSTELLATION GNSS RECEIVER CONFIGURATION

This section explain the performance of a single constellation GNSS (i.e., GPS) under the same constrained environments as used for the multi-constellation configuration, i.e., open-sky, half-sky and quarter-sky. Since, we are using GPS, the maximum visible satellites at any time of the day were found to be 11 with 9 averagely available to the receiver over the observation period. The GPS results are shown

in Fig. 9 for satellite geometry, availability and Blockage, reported position, precision and accuracy achieved for each candidate site/scenario during the same observation time $(06:00 - 12:00)$ as used for the multi-constellation configuration above.

The major difference between the single constellation and the multi-constellation configuration is the availability of satellites. In open-sky case, the average number of locked satellites reduced to 9 in Fig. 9(a) as compared to the multi-constellation case where 38 satellites were locked. Although, the position estimated in the open-sky case is accurate to almost 1m but the precision was not as the reported positions were moving away from the center of CEP and DRMS regions in Fig. 9(e) compared to multi-constellation were both CEP and DRMS were less than 1m (Fig. 7(e)). The mean of the position standard deviation in open-sky in Fig. 9(d) also increased to 1.42 m compared to 0.96 m in multi-constellation case. These results show that the precision and accuracy of single constellation systems is not as good as the multi-constellation case and satellite availability and geometry plays an important part in receiver's performance. When we moved on to half-sky and quarter-sky cases for the single constellation case, it is observed that the performance was highly compromised due to blockage, multipath and NLOS signal reception. In half-sky case in Fig. 9(b), out the of 6 hours, outages occurred for almost 3 hours and even when the receiver was giving positioning parameters there were large errors in the reported positions as can be seen in Fig. 9(c) in which the positioning values are scattered over a wider area giving a mean standard deviation of 18.2 m (Fig. 9(d)) which was only 3.4m in multi-constellation case. This resulted in the increase in CEP and DRMS circle radiuses to 16.7 m and 22.2 m respectively indicating that the receiver may report a positioning error of up to 17 m which was only 3.2 m in case
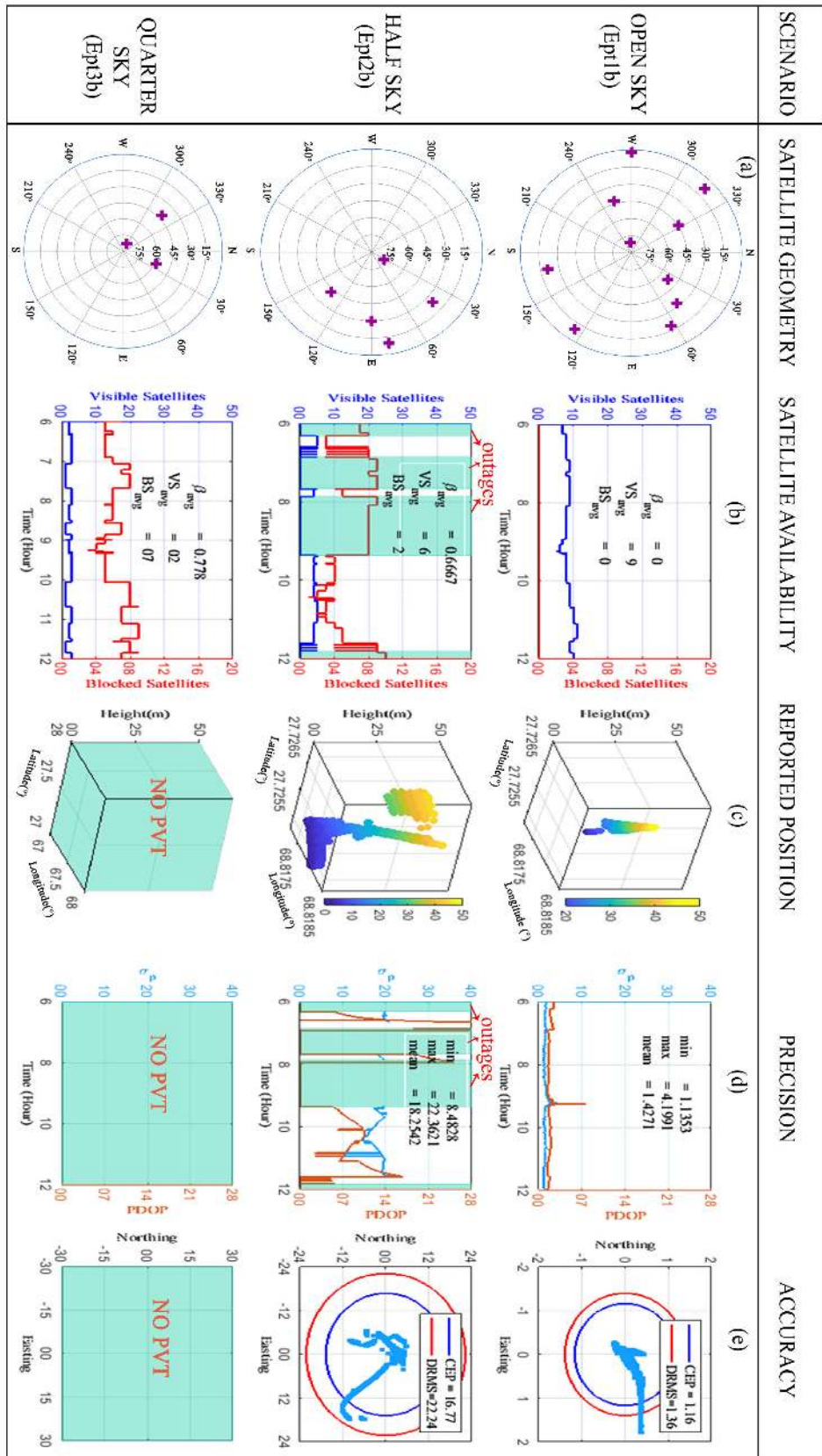
FIGURE 9. GPS Performance in open-sky, half-sky and quarter-sky: (a) Geometric distribution of satellites in orbit; (b) Satellite availability; (c) Reported position using latitude, longitude and height); (d) Precision in PDOP and σ_P; (e) Accuracy (CEP and DRMS).

of MCMF receiver configuration as shown in half-sky case in Fig. 7(e). On the other hand, in quarter-sky case, we only had 2 satellites locked by the receiver on average most of the time having NLOS reception and due to this the receiver did not give us any position in GPS case.

A table mentioning the summary of the positioning factors along with the accuracy and precision parameters are given in table 4. The table highlight the same factors which were also given for the multi-constellation case. A comparison is shown for the open-sky, half-sky and quarter-sky cases. This table gives a brief overview of the performance evaluation characteristics of a single constellation system. As obvious, precision and accuracy of single constellation system is much lower than the multi-constellation systems if we compare the σ_p, PDOP, CEP and DRMS in open-sky, half-sky or quarter-sky cases.

TABLE 4. Summary of the GPS receiver configuration in Open-Sky, Half-sky and Quarter-sky.

Scenario	Satellite Availability		Precision		Accuracy	
	VS mx/ag/mn	BS mx/ag/mn	σ_p mx/ag/mn	PDOP mx/ag/mn	CEP (m)	DRMS (m)
Open Sky	11/09/05	00/00/00	4.19/1.43/1.13	7.67/1.74/1.39	1.1662	1.3959
Half Sky	06/06/04	10/02/01	22.4/18.2/8.5	59.1/8.3/2.5	16.77	22.24
Quarter Sky	03/02/01	09/07/03	00/00/00	00/00/00	00	00

VS = Visible Satellites, BS = Blocked Satellites, σ_p = Position Standard Deviation, mx = maximum, ag = average, mn = minimum

VI. AN IMPROVED GNSS RECEIVER DESIGN BASED ON ADAPTIVE ENVIRONMENT NAVIGATION (AEN) ALGORITHM

A satellite-based navigation system is expected to provide positioning with acceptable level of accuracy at all times. However, based on the detailed analysis of single and multi-constellation GNSS configurations in this paper in low to highly dynamic multipath environments, it is established that GNSS performance (using one or more than one constellation) can vary greatly with the type of working environment. The combination of multiple navigation systems can improve the availability and accuracy but it cannot guarantee ubiquitous positioning and navigation, for instance, in our field experiments, multi-constellation GNSS using a combination of GPS, GLONASS, Galileo and Beidou resulted in outages for 43% of the time in the quarter-sky case. Hence, there must exist some reliable model by using which the performance of GNSS at receiver level can be further improved. In this regard, steps have been taken to significantly improve the availability of satellite-based PNT services in urban areas by increasing the number of satellites in orbit but this does not necessarily equate to more precise positioning in highly degraded environment (e. g., dense urban areas) due to significant impact of signal blockage and multipath or NLOS signals reception.

Several techniques have also been proposed to minimize the impact of MP/NLOS on positioning accuracy but most of these techniques treat MP/NLOS signals as unwanted interference and reject or de-weight them at antenna or receiver level [27], [50]–[53]. The exclusion of signals due to MP and NLOS can improve the positioning accuracy to some extent but it may lead to interruptions/outages in dense multipath environments having limited satellites availability. Therefore, it can be advantageous to incorporate these NLOS and/or multipath signals to avoid outages at the receiver [54]. This can be achieved by allowing wider bandwidth settings at receiver level through adaptive navigation based on environment characterization rather than using additional sensors or hardware's.

A GNSS receiver uses a code and carrier tracking loop [55], [56] to keep track of the detected satellites by obtaining the exact code phase and carrier frequency of the incoming GNSS signals respectively. Each of these loops is governed by the noise bandwidth which allows the amount of noise entered the tracking loop. Choosing a large noise bandwidth settings implies that the tracking loop would be able to handle wider dynamics and increased detection capability but with reduced efficiency. On the other hand, selecting a small noise bandwidth mean more accuracy due to less tracking error variance but the main disadvantage of using a small noise bandwidth is that, it is very sensitive to noise and a small increase may lead to signal loss of lock and thus is not recommended to use in dense multipath environments although most of the commercially available receivers use compact and fixed bandwidths to limit noise [55], [57], [58]. However, based on environment characterization, optimum noise bandwidth settings can be selected for a working environment which can increase the availability and accuracy.

Several researchers have used signal characteristics (i.e., No. of visible satellites, DOP and signal strength/CNR) to propose algorithms for environment detection using the machine learning techniques, fuzzy inference systems, stochastic modelling and Hidden Markov model [46]–[48], [59], [60]. In [46], Support Vector Machine (SVM) is used to achieve recognition accuracy of 89.3% across different environments using strength attenuation and strength fluctuation, blockage coefficient and GDOP as detection parameters. [47] has achieved overall environment detection accuracy of 88.2% using a hidden Markov model and two features i.e., satellite availability and signal strength. However, the main thing common in all of the previous work is that they are relying on signal strength or its variants, satellite availability and DOP to characterize the environment but, the signal strength many not properly contribute to environment detection in case of multi-constellation, multi-frequency configuration because: (1) multipath/NLOS reception can significantly affect the strength of signals but the severity of affect vary in frequencies [26]; (2) in case of multi-constellation, number of satellites will be more and monitoring huge number of satellites at signal level can result in huge processing load; (3) signal strength can be affected by lots of things
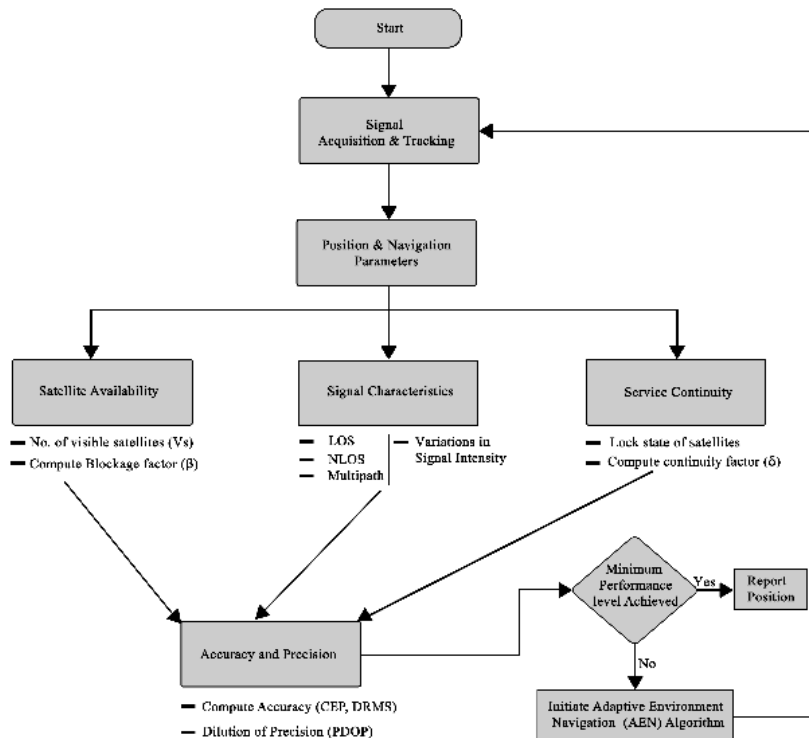
FIGURE 10. A complete workflow of the proposed AEN Method for GNSS position improvement in highly dynamic multipath environments.

including the low efficiency receiver or antenna and is also strongly associated with the elevation angle of the satellites. Hence, signal strength or its variants may not be an appropriate choice when using MCMF systems.

In this paper, a new Adaptive Environment based Navigation (AEN) algorithm is proposed for improved positioning availability and accuracy based on environment detection and characterization which is then tested using the MCMF receiver configuration. The main difference between AEN and previous models is that it does not uses signal strength as key parameter for environment detection and, instead uses availability and accuracy measures for environment detection and characterization. A complete workflow of the proposed AEN method is given below in Fig. 10. The factors used by the AEN method are satellites availability, blockage factor, continuity factor and PDOP. In Fig. 10, the AEN method starts by acquiring and then tracking all visible satellites in order to estimate the positioning and navigation parameters. It then calculates the blockage factor, continuity factor, PDOP and satellites visibility to check for CEP and DRMS to characterize the working environment into three distinct categories i.e., nominal/standard, partially degraded and highly dynamic multipath environment based on the set minimum performance level indicators Table 5 which can be used by the receiver to decide, when to initiate the adaptive tracking in case the working conditions have been changed. Table 5 can be intrepeted as follows: (1) in standard/nominal

environment, the satellites number tracked have to be greater than 30 but may vary based on how many systems are opted for navigation. The blockage factor, β must be less than 0.1, PDOP should be less than 1.5, $\sigma_p < 3$ m and CEP<2 m; (2) partially degraded environment where 15 to 30 satellites will be available that may or may not have direct LOS with the receiver. In this case, the following conditions need to be met for environment characterization, i.e., $0.1 < \beta < 0.5$, $1 <$PDOP< 3, $3m < \sigma_p < 5m$ and $2m <$CEP$< 5m$; (3) highly dynamic multipath environment in which less than 15 satellites are visible and only few will have direct LOS with the receiver. In this case, the following conditions need to be met for environment characterization, i.e., $\beta > 0.5$, PDOP> 3, $\sigma_p > 5m$ and $CEP > 5m$. These parameters may change in case the satellites in the constellation increases or if less than 4 systems are used for multi-constellation configuration. The implementation of the proposed AEN model given in Fig. 10 at receiver level is shown in Fig. 11. After estimating the positioning and navigation paramteres, the receiver starts working on the AEN moel for environment characterization using Table 5. If the conditions does not conform to present working environment then the receiver will move towards re-characterization of environment. Once the environment has been detected, the receiver tracking loop settings are updated based on whether the detected environment is standard/nominal, partially degraded or highly dynamic multipath.
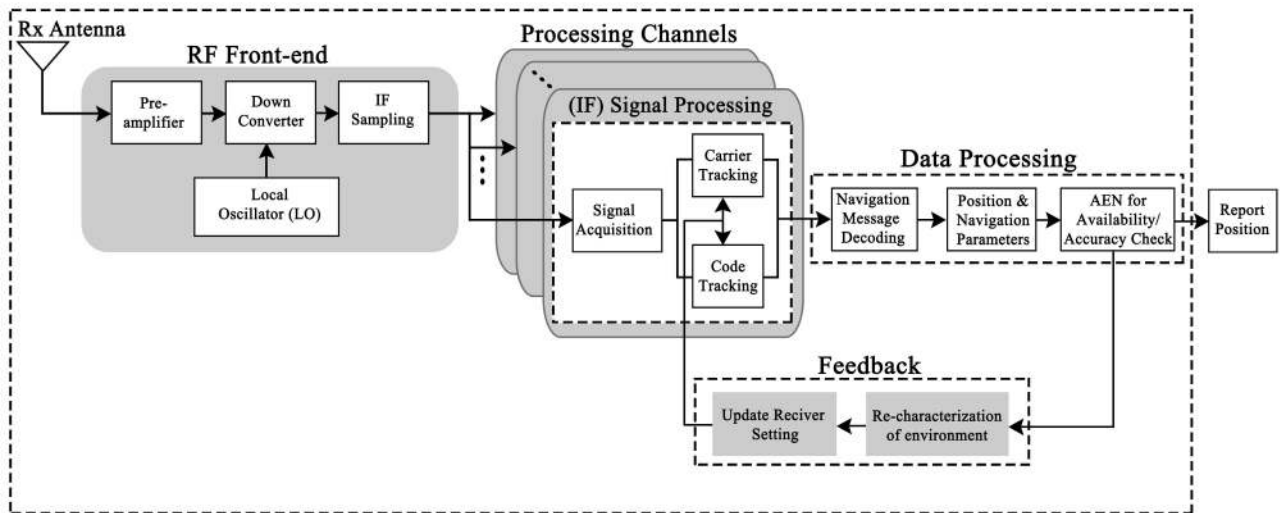
FIGURE 11. An improved GNSS receiver design based on AEN Algorithm.

TABLE 5. Minimum Performance level indicators for Environment Characterization using AEN.

Environment	Satellite Availability	Satellite Geometry	Accuracy/Positioning Error	Characteristics
Nominal/ Standard	Vs ≥ 30 β < 0.1	PDOP < 1.5	σ_p < 3 m CEP < 2m	Very low multipath Negligible disruption
Partially Degraded	15 < Vs < 30 0.1 ≤ β < 0.5	1.0 ≤ PDOP ≤ 3.0	3m ≤ σ_p < 10m 2m ≤ CEP ≤ 5m	Low/Medium multipath Some disruption
High dynamic multipath	Vs < 15 β > 0.5	PDOP > 3.0	σ_p > 10m CEP > 5m	High multipath Significant disruption

Vs – Visible Satellites (on average), β – Blockage Factor, σ_p – Position error (mean), CEP – Circular Error Probable

TABLE 6. AEN receiver model configuration for the highly dynamic multipath environment (i.e., quarter-sky).

| Parameter	Receiver Settings (without AEN)	Receiver Settings (with AEN)
Delay Lock Loop Bandwidth (Hz)	0.25	1
Phase Lock Loop Bandwidth (Hz)	15	15
Elevation Mask	10°	10°
C/N0 Mask (dB-Hz)	10	10
Data Collection Rate (Hz)	50	50
Continuity Factor (%)	57	94

In order to verify the working of the proposed AEN algorithm, it is tested in the quarter-sky case using a combination of 4 constellations, i.e., GPS, GLONASS, Galileo and Beidou. The open-sky and half-sky cases were not considered here as they were already giving good positioning solution and only a small improvement is expected in case the proposed model is applied on them using the MCMF configuration. The receiver tracking loop settings used in the quarter-sky case are given in Table 6. The last row in Table 6 shows the continuity factor achieved with and without using the AEN model which is more elaborately discussed through the field experiments. It should be noted that the modern receivers already have the capabilities of up-dating the acquisition and tracking loop parameters during runtime making it more easier to implement the proposed model. Regarding environment characterization and adaptive navigation, post-processing is used but it may also be incorporated during runtime directly into the receiver.

Results of the field experiments conducted in the highly dynamic multipath quarter-sky environment are shown in Fig. 12 which compares the positioning solution along with the satellite availability, continuity and Geometry of a multi-constellation GNSS receiver operating in standard mode without using the AEN model and the receiver incorporating the proposed AEN model. Fig. 12(a) shows the sky-view plot of the satellites. More satellites are locked after applying the AEN receiver model. This is more clearly shown in Fig. 12(b) through satellites locked versus the blocked satellites and the blockage coefficient β. The average number of satellites detected by standard GNSS receiver is 5 compared to 9 in case of the AEN receiver model. The β using AEN model fell by almost 11% showing increase in the satellites detected by the receiver for positioning solution. This shows that some of the satellites previously not tracked by the GNSS receiver without using AEN model just because of some extra noise could have been used to increase the positioning and GNSS availability. The positioning parameters,
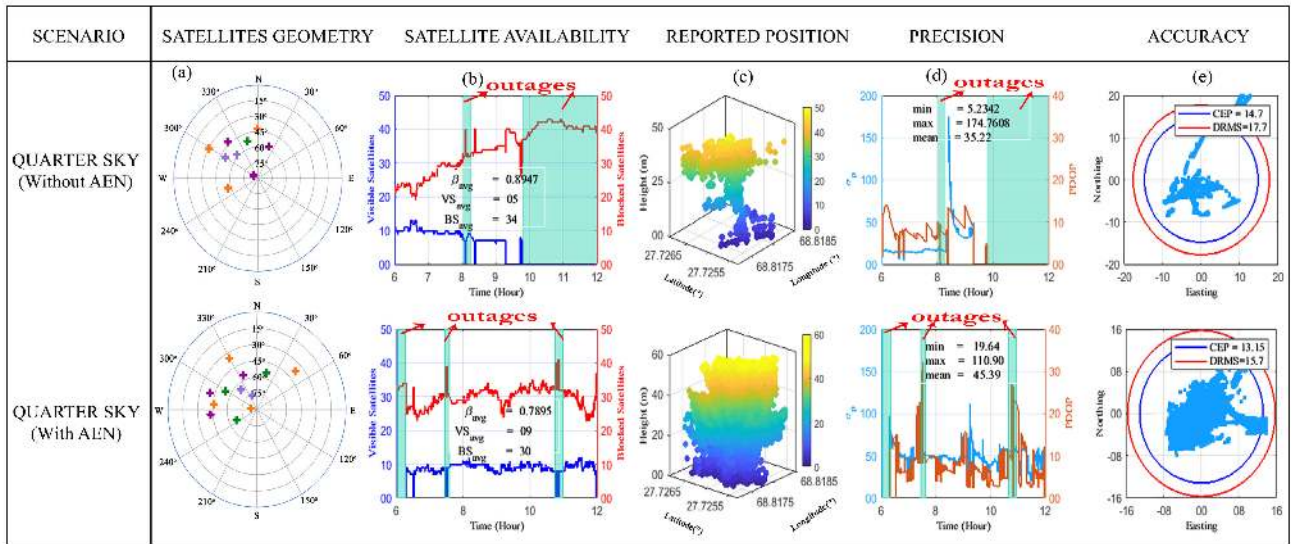
FIGURE 12. Performance comparison of a GNSS receiver in a highly dynamic mulitpath quarter-sky environment with and without using the AEN model. (a) Geometric distribution of satellites in orbit; (b) Satellite availability; (c) Reported position using latitude, longitude and height; (d) Precision in PDOP and σ_P; (e) Accuracy (CEP and DRMS).

i.e., latitude, longitude and height of the reported positions are shown in Fig. 12(c). The σ of the positioning along with the PDOP is shown in Fig. 12(d). The mean of σ in AEN is 35.2 compared to standard receiver having 45.3 as the mean of σ. Although, the mean of σ in case of AEN receiver is more than the standard receiver but the point to be noted here is that the non-AEN receiver model have positioning available only for about 3.5 hours out of 6 hours compared to AEN model where positioning is available for more than 5 hours. Further, the PDOP in case of AEN is mostly found to be less than 6 whenever the positioning is available compared to stadard receiver having PDOP of around 7 most of the time. Although, PDOP values in some cases are higher whenever there is more signal blockage and satellites constrained in a congested area. In terms of availability, the proposed AEN method proves to be a better candidate for navigation in highly dynamic multipath environments. To check the accuracy of the GNSS receiver with and without using the proposed AEN model, the CEP and DRMS are shown in Fig. 12(e) which can also be used for precision checking as well. In the AEN case, the CEP and DRMS have radiuses of 14.7 m and 17.7 m respectively which are reduced to 13.15 and 15.7 reducing the positioning error by almost 1.5 m overall. Further, based on the definition of precision and accuracy, it is observed that AEN approach tend to give more accurate positioning due to being revolve around the true position compared to standard receiver where the positioning points are spread apart leading to less accuracy and precision. So, after applying the proposed AEN model not only the availability is increased but also the accuracy and precision as well.

The satellite availability in terms of lock time of the satellites at Sig1 and Sig2 of the AEN receiver model is shown

in Fig. 13 for some of the satellite from GPS, GLONASS, GALILEO and BeiDou. The main thing to note here is that some of the satellites that were not detected during 09:45 to 12:00 hours without using the AEN receiver due to high multipath are now locked after using the AEN GNSS receiver. We have shown only those satellites that were locked by the receiver for more than half an hour rather than showing all the satellite although a minimum of 7 satellites were locked by the receiver at any given time when using AEN receiver. However, some of the satellites were losing lock very frequently due to multipath/NLOS and weak signal power which led to using only those satellites used for positioning by the receiver having strong signal power.

Fig. 14 shows the reported positions and outages occurred with and without using the AEN receiver model in a highly dynamic multipath quarter-sky environment. The pie-chart compares the percentage of availability (reported positions) versus the outages occurred during the position estimation period. Outages here means that less than 7 satellites were locked by the receiver and it failed to estimate position due to non-availability of PVT parameters. Reported position is the position in terms of latitude, longitue and height. The positions were recorded by the receiver for a continuous period of 6 hours having total of 216,000 epochs. Epcohs are the intervals at which the receiver logged the PVT parameters for position estimation. Here, the receiver logged 10 epochs in a second. Comparing the pie-charts of the AEN and non-AEN receiver models, it can be seen that AEN receiver gives position for 203,529 epochs out of 216,000 epochs and did not report position for 12,471 epochs which is almost 20 minutes of data. The one without using the AEN model reported positions only for 122,498 epochs out of 214,786 epochs logged by the receiver and outages occurred for 92,888 epochs which
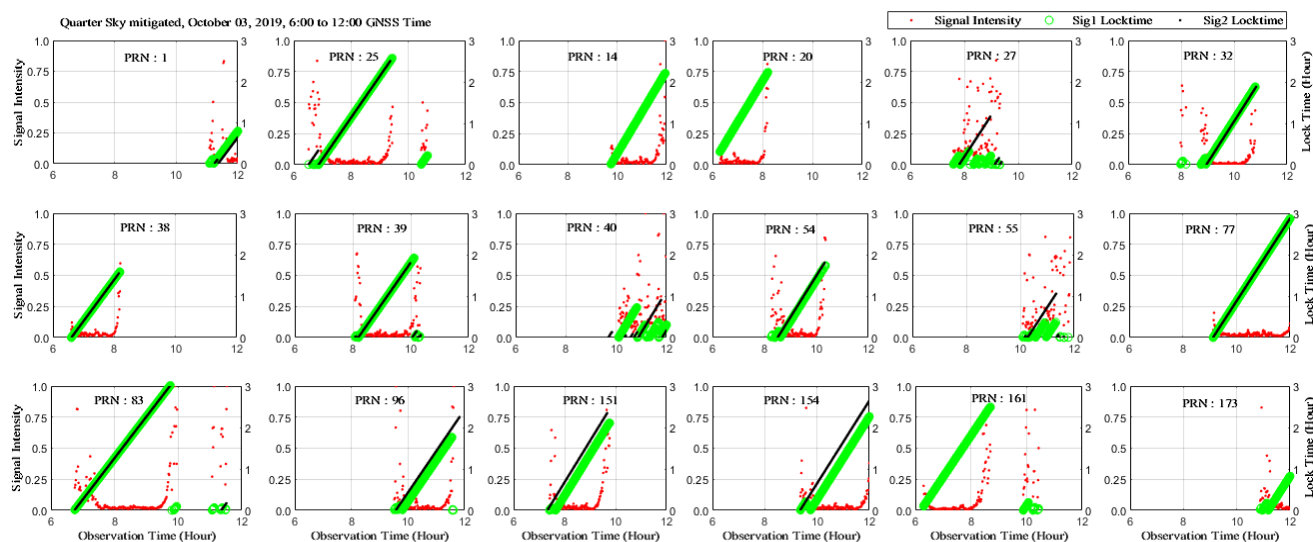
FIGURE 13. Signal intensity and lock time observed at Sig1 and Sig2 of the GNSS receiver employing AEN model.
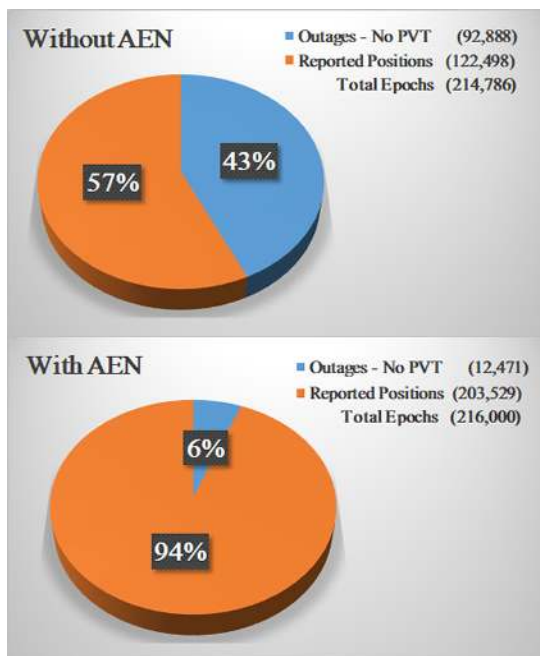

FIGURE 14. Reported positions and outages occurred with and without using the AEN receiver model in a highly dynamic mulitpath quarter-sky environment.

is almost 156 mintues of data. This comparison shows that the receiver without using the AEN model reported positions only 57% of the time which is increased to 94% when estimating the positioning using the AEN receiver model. This shows that the proposed AEN receiver model can be very effective when working in highly dynamic multipath environments tested using the MSMF configuration of 4 systems.

VII. CONCLUSION

This paper demonstrated that the quality of satellite signals available for positioning and navigation can be largely influenced by the environment in which a GNSS receiver is operating which not only affects the accuracy but also the precision in both the single and multi-constellation GNSS. Carefully planned field experiments in low, medium and highly dynamic multipath environments shows that the single constellation systems are more vulnerable to the environment changes as compared to the multi-constellation systems. Further, the precision and accuracy of multi-constellation systems in high multipath environments is found to be much better than the single constellation systems (i.e., GPS). It is therefore established that the multi-constellation GNSS systems can be a good candidate for dense urban environments having high multipath/NLOS signal reception. However, multipath/NLOS and blockage is still found to be a big problem even for the multi-constellation GNSS systems due to which availability, accuracy and precision and uninterrupted navigation services still may not be possible by using a GNSS receiver working in standard mode employing various multipath rejection techniques.

In order to overcome the availability, accuracy and precision problems for a multi-constellation GNSS, a new AEN algorithm has been presented in this paper which works on signal characteristic models to identify the environment based on low multipath, medium multipath and high multipath along with the blockage factor. The proposed AEN algorithm is then incorporated in a GNSS receiver to update the tracking loop parameters based on the minimum performance level indicators for the deteced envronment which resulted in the increased satellites availability, accuracy and precision in highly dynaminc multipath environments. A standard multi-constellation GNSS receiver working in a highly dynamic environment reported 43% outages which decreased to only 6% when using the AEN based GNSS receiver model. The blockage factor also decreased by almost 8%. Thus, based on the findings and performance comparison under different environments, it is concluded that the proposed

AEN based GNSS receiver model is a good candidate for improving the accruacy and availability of a GNSS which can be incorporated in real time without putting any extra burden on the receiver in terms of processing power or additional hardware modifications.

REFERENCES

[1] P. Brekke, "A day without satellites," in *Proc. 32nd Int. Tech. Meeting Satell. Division Inst. Navigat. (ION GNSS+)*, Miami, FL, USA, Oct. 2019, pp. 1–69.

[2] *GNSS Market Report*, Eur. Global Navigat. Satell. Syst. Agency (GSA), Prague, Czech Republic, 2019.

[3] C. Stallo, A. Neri, P. Salvatori, A. Coluccia, R. Capua, G. Olivieri, L. Gattuso, L. Bonenberg, T. Moore, and F. Rispoli, "GNSS-based location determination system architecture for railway performance assessment in presence of local effects," in *Proc. IEEE/ION Position, Location Navigat. Symp. (PLANS)*, Apr. 2018, pp. 374–381.

[4] J. Marais, J. Beugin, and M. Berbineau, "A survey of GNSS-based research and developments for the European railway signaling," *IEEE Trans. Intell. Transp. Syst.*, vol. 18, no. 10, pp. 2602–2618, Oct. 2017.

[5] P. Enge, "Satellite navigation: Present and future," in *Proc. 30th URSI Gen. Assem. Sci. Symp.*, Aug. 2011, pp. 1–4.

[6] X. Li, M. Ge, X. Dai, X. Ren, M. Fritsche, J. Wickert, and H. Schuh, "Accuracy and reliability of multi-GNSS real-time precise positioning: GPS, GLONASS, BeiDou, and galileo," *J. Geodesy*, vol. 89, no. 6, pp. 607–635, Jun. 2015.

[7] F. G. Toro, D. E. Diaz Fuentes, D. Lu, W. Tao, U. Becker, and B. Cai, "Accuracy analysis of BeiDou receivers for lane detection applications," in *Proc. IEEE/ION Position, Location Navigat. Symp. (PLANS)*, Apr. 2016, pp. 179–184.

[8] R. T. Ioannides, T. Pany, and G. Gibbons, "Known vulnerabilities of global navigation satellite systems, status, and potential mitigation techniques," *Proc. IEEE*, vol. 104, no. 6, pp. 1174–1194, Jun. 2016.

[9] D. Lu, S. Jiang, B. Cai, W. Shangguan, X. Liu, and J. Luan, "Quantitative analysis of GNSS performance under railway obstruction environment," in *Proc. IEEE/ION Position, Location Navigat. Symp. (PLANS)*, Apr. 2018, pp. 1074–1080.

[10] A. Stern and A. Kos, "Positioning performance assessment of geodetic, automotive, and smartphone GNSS receivers in standardized road scenarios," *IEEE Access*, vol. 6, pp. 41410–41428, 2018.

[11] L. Wang, P. D. Groves, and M. K. Ziebart, "Multi-constellation GNSS performance evaluation for urban canyons using large virtual reality city models," *J. Navigat.*, vol. 65, no. 3, pp. 459–476, Jul. 2012.

[12] J. Marek and L. Stepanek, "Accuracy and availability of the satellite navigation system GPS," in *Proc. 15th Conf. Microw. Techn. COMITE*, Apr. 2010, pp. 121–124.

[13] B. W. Parkinson, P. Enge, P. Axelrad, and J. J. Spilker, Jr., *Global Positioning System: Theory and Applications*, vol. 2. Reston, VI, USA: American Institute of Aeronautics and Astronautics, 1996.

[14] J. B. Tsui, "Satellite constelllation," in *Fundamentals of Global Positioning System Receivers: A Software Approach*. Hoboken, NJ, USA: Wiley, 2005, ch. 3, pp. 30–49.

[15] J. B. Tsui, "Basic GPS concept," in *Fundamentals of Global Positioning System Receivers: A Software Approach*. Hoboken, NJ, USA: Wiley, 2005, ch. 2, pp. 7–27.

[16] S. Bisnath and Y. Gao, "Precise point positioning," *GPS World*, vol. 20, no. 4, pp. 43–50, 2009.

[17] C. Cai, Y. Gao, L. Pan, and J. Zhu, "Precise point positioning with quad-constellations: GPS, BeiDou, GLONASS and galileo," *Adv. Space Res.*, vol. 56, no. 1, pp. 133–143, Jul. 2015.

[18] Q. Wu, M. Sun, C. Zhou, and P. Zhang, "Precise point positioning using dual-frequency GNSS observations on smartphone," *Sensors*, vol. 19, no. 9, p. 2189, May 2019.

[19] K. Su, S. Jin, and M. Hoque, "Evaluation of ionospheric delay effects on multi-GNSS positioning performance," *Remote Sens.*, vol. 11, no. 2, p. 171, Jan. 2019.

[20] W. Li, Y. Yuan, J. Ou, H. Li, and Z. Li, "A new global zenith tropospheric delay model IGGtrop for GNSS applications," *Chin. Sci. Bull.*, vol. 57, no. 17, pp. 2132–2139, Jun. 2012.

[21] A. D. Torre and A. Caporali, "An analysis of intersystem biases for multi-GNSS positioning," *GPS Solutions*, vol. 19, no. 2, pp. 297–307, Apr. 2015.

[22] J. Zidan, E. I. Adegoke, E. Kampert, S. A. Birrell, C. R. Ford, and M. D. Higgins, "GNSS vulnerabilities and existing solutions: A review of the literature," *IEEE Access*, early access, Feb. 13, 2020, doi: 10.1109/ACCESS.2020.2973759.

[23] N. Zhu, J. Marais, D. Betaille, and M. Berbineau, "GNSS position integrity in urban environments: A review of literature," *IEEE Trans. Intell. Transp. Syst.*, vol. 19, no. 9, pp. 2762–2778, Sep. 2018.

[24] A. Pirsiavash, A. Broumandan, G. Lachapelle, and K. O'Keefe, "GNSS code multipath mitigation by cascading measurement monitoring techniques," *Sensors*, vol. 18, no. 6, p. 1967, Jun. 2018.

[25] C. Chen, G. Chang, N. Zheng, and T. Xu, "GNSS multipath error modeling and mitigation by using sparsity-promoting regularization," *IEEE Access*, vol. 7, pp. 24096–24108, 2019.

[26] H. Wen, S. Pan, W. Gao, Q. Zhao, and Y. Wang, "Real-time single-frequency GPS/BDS code multipath mitigation method based on C/N0 normalization," *Measurement*, vol. 164, Nov. 2020, Art. no. 108075.

[27] P. D. Groves, Z. Jiang, B. Skelton, P. A. Cross, L. Lau, Y. Adane, and I. Kale, "Novel multipath mitigation methods using a dual-polarization antenna," in *Proc. 23rd Int. Tech. Meeting Satell. Division Inst. Navigat. (ION GNSS)*, Portland, OR, 2010, pp. 140–151.

[28] K. Palamartchouk, P. Clarke, S. Edwards, and R. Tiwari, "Dual-polarization gnss observations for multipath mitigation and better high-precision positioning," in *Proc. 28th Int. Tech. Meeting Satell. Division Inst. Navigat. (ION GNSS)*, Tampa, FL, USA, Sep. 2015, pp. 2772–2779.

[29] J. Li and Y. Wang, "GPS receiver failure detection method in high dynamic environment," in *Proc. IEEE/ION Position, Location Navigat. Symp. (PLANS)*, Apr. 2018, pp. 349–354.

[30] S. Tongleamnak and M. Nagai, "Simulation of GNSS availability in urban environments using a panoramic image dataset," *Int. J. Navigat. Observ.*, vol. 2017, pp. 1–12, Jan. 2017.

[31] P. Xie and M. G. Petovello, "Measuring GNSS multipath distributions in urban canyon environments," *IEEE Trans. Instrum. Meas.*, vol. 64, no. 2, pp. 366–377, Feb. 2015.

[32] NovAtel Inc., "GNSS error sources," in *An Introduction to GNSS GPS, GLONASS, BeiDou, Galileo and other Global Navigation Satellite Systems*. Calgary, AB, Canada: NovAtel Inc., 2015, ch. 4, pp. 46–48.

[33] O. Osechas, K. Kim, K. Parsons, and Z. Sahinoglu, "Detecting multipath errors in terrestrial GNSS applications," in *Proc. Int. Tech. Meeting Inst. Navigat.*, 2015, pp. 465–474.

[34] Y. T. Morton, F. Van Graas, Q. Zhou, and J. Herdtner, "Assessment of the higher order ionosphere error on position solutions," *Navigation*, vol. 56, no. 3, pp. 185–193, Sep. 2009.

[35] T. A. Skidmore and F. van Graas, "An investigation of tropospheric errors on differential GNSS accuracy and integrity," in *Proc. 17th Int. Tech. Meeting Satell. Division Inst. Navigat. (ION GNSS)*, 2001, pp. 2752–2760.

[36] I. G. Petrovski, *Standalone Positioning With GNSS*. Cambridge, U.K.: Cambridge Univ. Press, 2014, p. 88–109.

[37] D. Tang, D. Lu, B. Cai, and J. Wang, "GNSS localization propagation error estimation considering environmental conditions," in *Proc. 16th Int. Conf. Intell. Transp. Syst. Telecommun. (ITST)*, Oct. 2018, pp. 1–7.

[38] J. Januszewski, "Geometry and visibility of satellite navigation systems in restricted area," in *Proc. Nat. Tech. Meeting Inst. Navigat.*, 2001, pp. 827–839.

[39] J. Fernow and D. O'Laughlin, "Estimating continuity of GNSS," in *Proc. 17th Int. Tech. Meeting Satell. Division Inst. Navigat. (ION GNSS)*, 2001, pp. 2113–2123.

[40] F. van Diggelen. *GPS Accuracy: Lies, Damn Lies, and Statistics*. Accessed: Jan. 20, 2020. [Online]. Available: https://www.GPSworld.com/GPSGNSS-accuracy-lies-damn-lies-and-statistics-1134/

[41] T. Szot, C. Specht, M. Specht, and P. S. Dabrowski, "Comparative analysis of positioning accuracy of samsung galaxy smartphones in stationary measurements," *PLoS ONE*, vol. 14, no. 4, Apr. 2019, Art. no. e0215562.

[42] Novatel. *GPS Position Accuracy Measures*. [Online]. Available: https://www.novatel.com/assets/Documents/Bulletins/apn029.pdf

[43] M. Tahsin, S. Sultana, T. Reza, and M. Hossam-E-Haider, "Analysis of DOP and its preciseness in GNSS position estimation," in *Proc. Int. Conf. Electr. Eng. Inf. Commun. Technol. (ICEEICT)*, May 2015, pp. 1–6.

[44] (2019). *Septentrio PolaRx5S User Manual*. Accessed: Mar. 3, 2019. [Online]. Available: https://www.septentrio.com/en/products/GNSS-receivers/reference-receivers/polarx5s

[45] (2019). *PolaNt Choke Ring B3/E6 Data sheet*. Accessed: Mar. 3, 2019. [Online]. Available: https://www.septentrio.com/en/products/accessories/antennas/chokering-b3-e6

[46] Y. Wang, P. Liu, Q. Liu, M. Adeel, J. Qian, X. Jin, and R. Ying, "Urban environment recognition based on the GNSS signal characteristics," *Navigation*, vol. 66, no. 1, pp. 211–225, 2019.

[47] H. Gao and P. D. Groves, "Environmental context detection for adaptive navigation using GNSS measurements from a smartphone," *Navigation*, vol. 65, no. 1, pp. 99–116, Mar. 2018.

[48] P. D. Groves, H. Martin, K. Voutsis, D. Walter, and L. Wang, "Context detection, categorization and connectivity for advanced adaptive integrated navigation," in *Proc. 26th Int. Tech. Meeting Satell. Division Inst. Navigat. (ION GNSS+)*, Nashville, TN, USA, Sep. 2013, pp. 1039–1056.

[49] L.-T. Hsu, "Analysis and modeling GPS NLOS effect in highly urbanized area," *GPS Solutions*, vol. 22, no. 1, p. 7, Jan. 2018.

[50] L.-T. Hsu, H. Tokura, N. Kubo, Y. Gu, and S. Kamijo, "Multiple faulty GNSS measurement exclusion based on consistency check in urban canyons," *IEEE Sensors J.*, vol. 17, no. 6, pp. 1909–1917, Mar. 2017.

[51] C. Pinana-Diaz, R. Toledo-Moreo, D. Bétaille, and A. F. Gomez-Skarmeta, "GPS multipath detection and exclusion with elevation-enhanced maps," in *Proc. 14th Int. IEEE Conf. Intell. Transp. Syst. (ITSC)*, Oct. 2011, pp. 19–24.

[52] P. D. Groves, Z. Jiang, M. Rudi, and P. Strode, "A portfolio approach to NLOS and multipath mitigation in dense urban areas," in *Proc. 26th Int. Tech. Meeting Satell. Division Inst. Navigat. (ION GNSS+)*, Nashville, TN, USA, Sep. 2013, pp. 3231–3247.

[53] J. Lesouple, T. Robert, M. Sahmoudi, J.-Y. Tourneret, and W. Vigneau, "Multipath mitigation for GNSS positioning in an urban environment using sparse estimation," *IEEE Trans. Intell. Transp. Syst.*, vol. 20, no. 4, pp. 1316–1328, Apr. 2019.

[54] G. X. G. Yuting Ng. *Position Estimation Using Non-Line-of-Sight GPS Signals*. Accessed: Jan. 20, 2020. [Online]. Available: https://www.GPSworld.com/GPSGNSS-accuracy-lies-damn-lies-and-statistics-1134/

[55] K. Borre, D. M. Akos, N. Bertelsen, P. Rinder, and S. H. Jensen, "Carrier and code tracking," in *A software-Defined GPS and Galileo Receiver: A Single-Frequency Approach*. New York, NY, USA: Birkhäuser, 2007, ch. 7, pp. 87–107.

[56] A. Alaqeeli, J. Starzyk, and F. van Graas, "Real-time acquisition and tracking for GPS receivers," in *Proc. Int. Symp. Circuits Syst. (ISCAS)*, vol. 4, 2003, p. 4.

[57] E. Kaplan and C. Hegarty, "Satellite signal acquisition, tracking, and data demodulation," in *Understanding GPS: Principles and Applications*. Norwood, MA, USA: Artech House, 2005, ch. 5, pp. 153–240.

[58] A. J. Van Dierendonck, P. Fenton, and T. Ford, "Theory and performance of narrow correlator spacing in a GPS receiver," *Navigation*, vol. 39, no. 3, pp. 265–283, Sep. 1992.

[59] L.-T. Hsu, Y. Gu, and S. Kamijo, "Intelligent viaduct recognition and driving altitude determination using GPS data," *IEEE Trans. Intell. Vehicles*, vol. 2, no. 3, pp. 175–184, Sep. 2017.

[60] N. M. Drawil, H. M. Amar, and O. A. Basir, "GPS localization accuracy classification: A context-based approach," *IEEE Trans. Intell. Transp. Syst.*, vol. 14, no. 1, pp. 262–273, Mar. 2013.

ARSLAN AHMED received the M.S. degree in communication engineering from The University of Manchester, U.K., in 2010, and the Ph.D. degree in electrical engineering from Newcastle University, U.K., in 2015, with a major in GNSS Receiver designing and space weather effects on GNSS. From 2011 to 2015, he worked on Engineering and Physical Sciences Research Council (EPSRC), U.K., Project on Space Weather Effects on Navigation Systems and its Mitigation. Since 2016, he has been working as an Assistant Professor with the Department of Electrical Engineering, Sukkur IBA University, Pakistan. He has several conference and journal publications in GNSS related areas and has also given keynote talks at several international forums on GNSS. His research interests include ionospheric scintillation, GNSS Receiver designing and optimization, and GNSS vulnerabilities in urban environment. He also developed the first ever GNSS and Space Weather Laboratory in Pakistan with the help of government funding.

HINA MAGSI received the B.E. degree in telecommunication engineering from the Mehran University of Engineering and Technology, Jamshoro, in 2016, and the M.S. degree in electronics and communication from Sukkur IBA University, Pakistan. She is currently pursuing the Ph.D. degree with the Department of Electrical Engineering, Sukkur IBA University. She is also a Research Associate with the Department of Electrical Engineering, Sukkur IBA University, working on HEC NRPU Project (Ionospheric Scintillation Monitoring and Detection over Pakistan and its Mitigation). Her research interests include precise positioning and navigation, ionospheric scintillation monitoring and detection, and signal acquisition and processing.

ARIF HUSSAIN received the B.E. degree in electronics engineering and the master's degree in electrical engineering with a specialization in GNSS and autonomous navigation from the Department of Electrical Engineering, Sukkur IBA University, Pakistan, in 2017 and 2020, respectively. Since 2018, he has been working as a Research Associate with the GNSS and Space Weather Laboratory, Sukkur IBA University, Pakistan. He has published analysis at many platforms on Space Weather effects on GNSS by analyzing scintillation occurrence patterns over Pakistan. His research interests include autonomous navigation architectures, GNSS accuracy and precision, environment characterization, and adaptive tracking loops for GNSS receivers.

RAJESH TIWARI received the Ph.D. degree from Barkatullah University, India. He worked as a Graduate Research Assistant with the University of Calgary, Canada. He is currently a Senior Navigation Engineer and an Honorary Fellow of the University of Nottingham, Nottingham, U.K. He is also a Research Associate and a Teaching Fellow of Newcastle University, U.K. His research interests include GNSS signal processing, GNSS software defined receiver, and sensor fusion for the autonomous vehicle. He is also involved in designing integrity solutions for the autonomous vehicles at Nottingham Scientific Limited, Nottingham. He is a Fellow of Higher Education Academy. He was involved in Antarctic Scientific Expedition to investigate the space weather phenomena and its effect on GNSS signals in the Antarctic region. He also received the Prestigious International Young Scientist Award, URSI, the Best Paper Presentation Award ION, USA, and many best lecturer awards from Newcastle University.

●●●